Optimized Double-well quantum interferometry with Gaussian-squeezed states

Y. P. Huang and M. G. Moore
Department of Physics & Astronomy, Michigan State University, East Lansing, MI 48824

A Mach-Zender interferometer with a gaussian number-difference squeezed input state can exhibit sub-shot-noise phase resolution over a large phase-interval. We obtain the optimal level of squeezing for a given phase-interval $\Delta\theta_0$ and particle number N, with the resulting phase-estimation uncertainty smoothly approaching $3.5/N$ as $\Delta\theta_0$ approaches $10/N$, achieved with highly squeezed states near the Fock regime. We then analyze an adaptive measurement scheme which allows any phase on $(-\pi/2, \pi/2)$ to be measured with a precision of $3.5/N$ requiring only a few measurements, even for very large N. We obtain an asymptotic scaling law of $\Delta\theta \approx (2.1+3.2\ln(\ln(N_{tot}\tan\Delta\theta_0)))/N_{tot}$, resulting in a final precision of $\approx 10/N_{tot}$. This scheme can be readily implemented in a double-well Bose-Einstein condensate system, as the optimal input states can be obtained by adiabatic manipulation of the double-well ground state.

PACS numbers: 03.75.Dg,03.75.Lm,42.50.Dv

Measuring an arbitrary phase with precision well above the standard quantum limit (SQL), i.e., below shot-noise, has been a long-standing challenge in quantum interferometry [1, 2, 3, 4]. The SQL minimum phase uncertainty is $1/\sqrt{N_{tot}}$, but the theoretical lower limit to the phase uncertainty, known as the Heisenberg limit (HL), is $1/N_{tot}$, where N_{tot} is the total number of particles used in the determination of the phase. There have been many proposals to achieve $1/N_{tot}$ scaling in a two-input interferometer, which are based on number-difference squeezed input states [1, 2, 3, 5], coherent and/or squeezed vacuum input states [6, 7, 8], or the maximally-entangled N-particle NOON state, $\frac{1}{2}(|N,0\rangle + |0,N\rangle)$ [9, 10, 11, 12]. Recently, the double-well Bose-Einstein condensate (BEC) has emerged as a promising system for high-precision matter-wave interferometry [13, 14, 15, 16, 17], including progress towards atom-counting at the single-particle level [18, 19]. For this system, the squeezed-vacuum protocols are not applicable, while the NOON state is not suited to determine an unknown phase due to the periodicity of the phase-distribution [20, 21]. This leaves number-difference squeezed states as a viable candidate, although to date there has been no systematic study of how to measure arbitrary phases at or near HL precision in the large-N limit. In this Letter we perform such an analysis and show that an asymptotic scaling of $(\ln(\ln N_{tot}))/N_{tot}$ can be achieved via multiple adaptive measurements with Gaussian number-squeezed states, which can be readily created in a double-well BEC.

For measuring a phase of $\theta = 0$, it has been shown that the Twin-Fock (TF) state, and the related Pezze-Smerzi (PS) state can achieve Heisenberg scaling [20, 22, 23, 24]. We find, however, for $\theta \neq 0$ the phase-uncertainty of the TF and PS states rapidly decay to worse-than-SQL, and in the limit of large N approach constant values, independent of N. While the PS state was only investigated for $\theta = 0$, Kim *et al* [24] investigated $\theta \neq 0$ for the TF state with $N = 100$. They claim a phase uncertainty $\sim 1/N_{tot}$ for $\theta < 1/N$, and growing rapidly thereafter. Our results similarly indicate that the TF and PS states become worse than shot-noise for $\theta \gg 1/N$.

To find the optimal input state, we constrain ourselves to the ground-states of a double-well BEC with repulsive interactions for experimental obtainability. The double-well BEC system is described by the Hamiltonian,

$$\hat{H}(\chi) = -2\tau\hat{J}_x + \delta\hat{J}_z + U\hat{J}_z^2, \tag{1}$$

where τ is the inter-well tunneling rate, U is the atom-atom interaction strength, and δ is the asymmetric tilt of the double-well, presumably due to the external perturbation being measured. The angular momentum operators are defined as $\hat{J}_x = \frac{1}{2}(\hat{c}_L^\dagger\hat{c}_R + \hat{c}_R^\dagger\hat{c}_L)$, $\hat{J}_y = \frac{1}{2i}(\hat{c}_L^\dagger\hat{c}_R - \hat{c}_R^\dagger\hat{c}_L)$ and $\hat{J}_z = \frac{1}{2}(\hat{c}_L^\dagger\hat{c}_L - \hat{c}_R^\dagger\hat{c}_R)$, with $\hat{c}_L, \hat{c}_R$ being the annihilation operators for particles in the two localized modes. For repulsive atom-atom interaction, and $\delta \approx 0$ the ground state is very close to a Gaussian squeezed (GS) state of the form $|\sigma\rangle \propto \sum_{n=-N/2}^{N/2} e^{-n^2/4\sigma^2}|n\rangle$, where $|n\rangle$ is a number-difference eigenstate satisfying $\hat{J}_z|n\rangle = n|n\rangle$. The width σ, depends on the parameter $u = U/\tau$, and is given by $\sigma^2 = N/4\sqrt{1+uN}$ [25]. The nature of our adaptive measurement scheme requires that we tune u to an optimal value which takes into account our prior knowledge of N and θ, thus we have $u \to u(N,\theta)$. This tuning is accomplished by varying U/τ via a Feshbach resonance and/or changing the shape of the double-well potential, and allows σ to be varied between 0 and $\sqrt{N}/2$, corresponding to maximal number-difference squeezing and no squeezing, respectively.

To implement a Mach-Zehnder interferometer (MZI), we set $U = 0$ and allow tunneling for $t = \pi/4\tau$ duration, thus realizing a linear 50/50 beamsplitter, described by the propagator $e^{i\frac{\pi}{2}\hat{J}_x}$. This is followed by a sudden raising of the potential barrier to turn off tunneling and allow phase acquisition due to the small but non-vanishing δ. Holding the system for a measurement time T, a phase shift of $\theta = -\delta T$ will be acquired, described by the prop-

agator $e^{i\theta \hat{J}_z}$. The barrier is then lowered again to implement a second beamsplitter.

In the MZI, a symmetric input state $|\Psi_{in}\rangle$ is transformed into the phase-dependent output state $|\Psi_{out}\rangle = e^{i\frac{\pi}{2}\hat{J}_x}e^{i\theta\hat{J}_z}e^{i\frac{\pi}{2}\hat{J}_x}|\Psi_{in}\rangle = e^{-i\theta\hat{J}_y}e^{i\pi\hat{J}_x}|\Psi_{in}\rangle$ [1]. Applying this transformation to a typical GS state, results in an output state whose properties are easily understood using the Bloch sphere quasi-probability distribution [5], which assigns a probability to each point on a sphere of radius $N/2$ according to $P(\theta,\phi) = |\langle N/2|e^{i\hat{J}_y(\pi/2-\theta)}e^{i\hat{J}_z\phi}|\Psi_{out}\rangle|^2$. Note any N-atoms state for which all atoms are in the same single-particle state can be written in the form $e^{-i\hat{J}_z\phi}e^{-i\hat{J}_y(\pi/2-\theta)}|N/2\rangle$, which has eigenvalue $N/2$ with respect to the projection of $\vec{J}$ onto the axis defined by θ,ϕ. In this picture, the TF and PS states are thin equatorial rings, and a GS input state is an ellipse centered on the J_x axis, compressed along the J_z-direction. Typical GS input and output states are shown in figure 1(a).

Phase information is obtained by measuring the number difference between the two interferometer modes, which projects the output state onto a $\hat{J}_z$ eigenstate. Quantum fluctuations in this measurement are governed by the projection of the output distribution onto the J_z-axis. Due to the rigid rotation, the width of the projection will be determined by a θ-dependent combination of the J_z and J_x noise of the input distribution. The goal of this paper is thus to find the optimal amount of squeezing to minimize the phase uncertainty given a fixed particle number N and an initial estimated phase θ_0 with uncertainty $\Delta\theta_0$.

Before we present numerical results from a rigorous Bayesian analysis, we first use linearized error propagation to provide an approximate analytical description of the interferometer performance. An analytical result is important for predicting the behavior at large N, where a numerical result is inaccessible. In this approach, the phase uncertainty is estimated by evaluating $\Delta\theta = [\partial\langle\hat{J}_z\rangle/\partial\theta]^{-1}\Delta J_z$ at the interferometer output. For input states symmetric around $n=0$, the expectation values at the output are related to those at the input via $\langle\hat{J}_z\rangle = \sin\theta\langle\hat{J}_x^i\rangle$ and $\Delta J_z = \sqrt{\cos^2\theta\Delta {J_z^i}^2 + \sin^2\theta\Delta {J_x^i}^2}$. For GS states, $\langle\hat{J}_x^i\rangle \approx N/2$, and $\Delta J_z^i = \sigma$, which immediately leads to $\langle\hat{J}_z\rangle = N(\sin\theta)/2$. In figure 1(c) we see that $\Delta J_x^i \approx N/2 - \sqrt{N^2/4 - \Delta {J_y^i}^2}$. Since GS state is a minimum uncertainty state with $\Delta J_y^i \Delta J_z^i = \langle\hat{J}_x^i\rangle/2$, we see that $\Delta J_y^i = N/4\sigma$. This leads to $\Delta J_x^i = \alpha N/\sigma^2$, with $\alpha \approx 0.06$. Exact numerical calculations verify this analytic form for $1 \ll \sigma \ll \sqrt{N}/2$, as shown in figure 1(d), but with $\alpha = 0.09$. Inserting these results into the error-propagation formula, we find

$$\Delta\theta \approx \frac{2\sigma}{N}\sqrt{1+\left[\frac{0.09N\tan\theta}{\sigma^3}\right]^2}. \qquad (2)$$

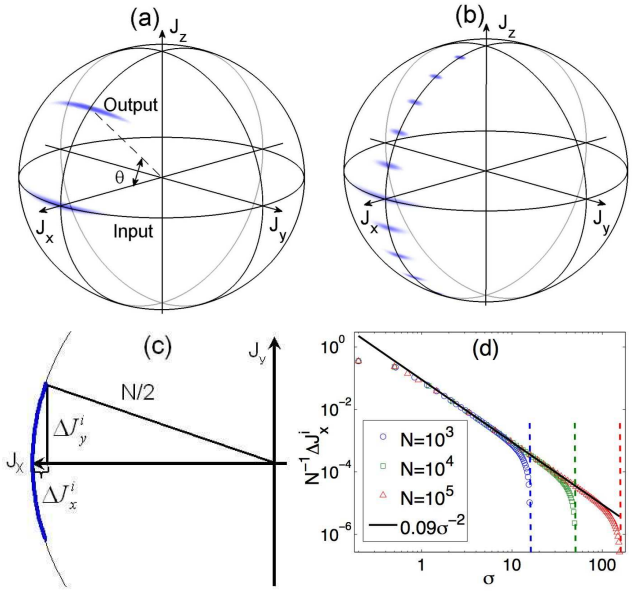

FIG. 1: (Color online) Bloch-sphere analysis of the MZI with a GS input state: (a) A typical GS state at input and output stages; (b) output states for optimized input states with $\theta = 0, \pm\frac{\pi}{12}, \pm\frac{\pi}{6}, \pm\frac{\pi}{4}, \pm\frac{\pi}{3}, \pm\frac{5\pi}{12}$; (c) geometric origin of the J_x input noise, ΔJ_x^i; (d) numerical results plotting $\Delta J_x^i/N$ versus σ on a log-log scale for three different N-values, validating the functional form of ΔJ_x^i derived geometrically from (c). The dashed vertical lines correspond to $\sigma = \frac{\sqrt{N}}{2}$, where ΔJ_x^i drops to zero.

The TF and PS states roughly correspond to a fixed $\sigma \lesssim 1$, resulting in $\lim_{N\to\infty}\Delta\theta = .18\tan\theta/\sigma^2$, which quickly becomes saturated to an N-independent constant for $\theta \gg 1/N$, a result we have verified numerically with exact Bayesian calculations. On the other hand, if holding u fixed so that $\sigma \sim N^{1/4}$, the phase uncertainty scales as $\Delta\theta \sim 1/N^{3/4}$ for $\theta = 0$, as discussed in [26], and would eventually saturate to $\sim 1/\sqrt{N}$ for $\theta \neq 0$. Rather than holding σ or u fixed, we propose varying u and thus σ with N in order to minimize the phase variance. By setting $d\Delta\theta/d\sigma = 0$ we find

$$\sigma_{min}(\theta,N) \approx .503(N\tan|\theta|)^{1/3}, \qquad (3)$$
$$\Delta\theta_{min}(\theta,N) \approx 1.23(\tan|\theta|)^{1/3}/N^{2/3} \qquad (4)$$

From self-consistency, these expressions are valid only when $10/N \lesssim |\theta| \lesssim \tan^{-1}(.137\sqrt{N}) \approx \pi/2$.

We now employ rigorous Bayesian analysis to quantify the phase uncertainty and validate our approximate analytic results, again assuming that $|\theta|$ is not too close to $\pi/2$. According to Bayes theorem, upon a measurement result n_m, the probability that the actual phase is ϕ is $P(\phi|n_m) = P(n_m|\phi)/\int d\theta P(n_m|\theta)$, where $P(n|\theta) = |\langle n|e^{-i\theta\hat{J}_y}|\psi_{in}\rangle|^2$. The error-propagation result (4) is very close to the 68% confidence interval of $P(\phi|n)$ because the underlying number distribution of the optimized GS

output state is well approximated by the gaussian distribution $P(n|\theta) \approx [\sqrt{2\pi}\Delta n]^{-1} e^{-(n-N\sin\theta/2)/2\Delta n^2}$, where $\Delta n = \sqrt{1+\frac{\tan^2\theta}{2\tan^2\theta_a}}\sigma_{min}(\theta_a, N)$, with θ being the unknown phase, and θ_a being the assumed phase used for optimization. Provided that $|\theta| \sim |\theta_a|$, the dependence on θ is weak, and we have $\Delta n \approx \sqrt{3/2}\sigma_{min}(\theta_a, N)$. This shows that the most-probable outcome is $\bar{n} = N\sin\theta/2$, which is sensitive to the sign of θ. Because Δn is only weakly dependent on θ, the inverted distribution $P(\phi|n)$ will also be close to Gaussian in the small-angle regime, with width given by (4). To make a theoretical performance analysis for a fixed θ, we average over all possible measurement outcomes, defining $P(\phi|\theta) = \sum_n P(\phi|n)P(n|\theta)$ [22, 23]. This can be interpreted as the probability for an experimenter to infer ϕ given a true phase-shift of θ. The phase uncertainty $\Delta\theta$ is then defined as the 68% confidence interval, via $\int_{\theta-\Delta\theta}^{\theta+\Delta\theta} d\phi\, P(\phi|\theta) = .68$.

Using this approach, together with the exact double-well ground-state, we numerically find u_{min}, the value of U/τ which minimizes the phase uncertainty. In figure 2(a), we plot the corresponding $\sigma_{min} = \sigma(u_{min})$ as a function of N for several θs. Also shown is a least-squares fit to the $N > 10^3$ data (including many data points not shown explicitly) to the analytic form (3), giving

$$\sigma_{min}(\theta, N) = \begin{cases} 1.00, & |\theta| < 10/N; \\ 0.45(N\tan|\theta|)^{1/3}, & |\theta| > 10/N, \end{cases} \quad (5)$$

in good agreement with our analytical result. Inverting Eq. (5) to leads to

$$u_{min}(\theta, N) = \begin{cases} \frac{N}{16} - \frac{1}{N}, & |\theta| < 10/N; \\ \frac{1.52}{(\tan|\theta|)^{4/3}N^{1/3}} - \frac{1}{N}, & |\theta| > 10/N. \end{cases} \quad (6)$$

In Fig. 2(b) we plot the corresponding minimized $\Delta\theta_{min}$ versus N for several phases, achieved by setting $\sigma = \sigma_{min}(\theta, N)$. Again fitting the $N > 10^3$ data to the analytic form of (4), we find

$$\Delta\theta_{min}(\theta, N) = \begin{cases} 3.50/N, & |\theta| < 10/N; \\ 1.63(\tan|\theta|)^{1/3}/N^{2/3}, & |\theta| > 10/N. \end{cases} \quad (7)$$

The difference between the prefactor here and (4) is primarily due to a factor of approximately $\sqrt{2}$ which comes from the definition of $P(\phi|\theta)$.

In practice, θ is not known a-priori, hence it is not clear what value for θ to use in determining $\sigma_{min}(\theta, N)$ via Eq. (5). If we assume prior knowledge of the form $P(\theta) \propto \exp[-(\theta-\theta_0)^2/2\Delta\theta_0^2]$, we should first remove θ_0 by adding θ_0/T to the tilt δ during phase acquisition, and then use $\sigma_{min}(\Delta\theta_0, N)$. After obtaining a measurement result n_1, the estimated uncertainty $\Delta\theta_1$ is then be determined via $\int_{\theta_1-\Delta\theta_1}^{\theta_1+\Delta\theta_1} d\theta' P(\theta'|n_1)$, with $P(\theta'|n_1)$ being given by Bayes theorem. This will result in $\Delta\theta_1 \sim \Delta\theta_{min}(\Delta\theta_0, N)$. Based on Eq. (7), this uncertainty appears to scale only as $N^{-2/3}$, only a slight improvement of $N^{1/6}$ over the SQL. However, in many applications requiring high precision, the phases are very small, in which case the phase uncertainty can be reduced considerably due to the explicit phase dependence in (7). This is in contrast to a shot-noise-limited interferometer, where $\Delta\theta = 1/\sqrt{N}$ for all θs not too close to $\pm\pi/2$. The explicit theta-dependence in the optimized scheme is due to the fact that stronger number-squeezing can be tolerated at smaller angles before the $\hat{J}_x^i$ noise becomes detrimental. For example, if the phase is known to be smaller than $1/\sqrt{N}$, we have $\Delta\theta_{min} \leq 1.63/N^{5/6}$, which is now an $N^{1/3}$ improvement over the SQL. As can be seen from Eq. (7), a maximum sensitivity of $3.5/N$ can be achieved for $|\theta| < 10/N$, which is true Heisenberg scaling.

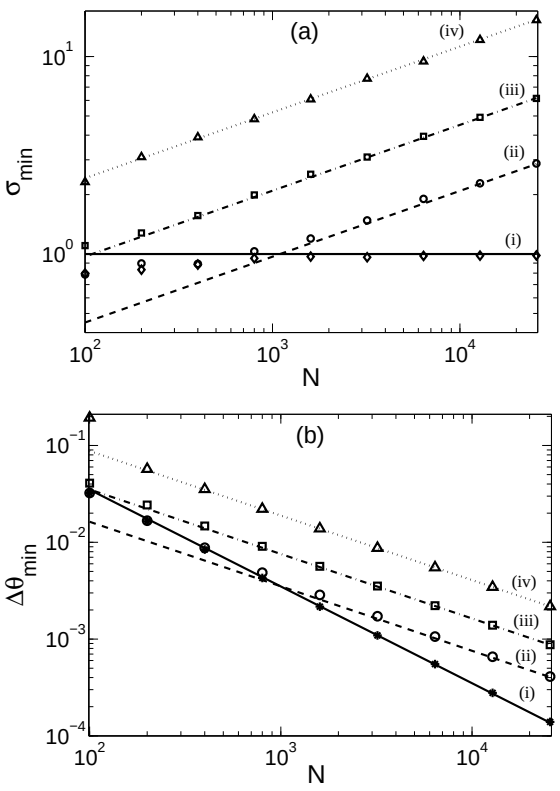

FIG. 2: Figure (a): Optimal width σ_{min} versus N for different θ; (b): corresponding minimized phase uncertainty $\Delta\theta_{min}$. In both figures, from (i) to (iv) the interferometer phases are $\theta = 0,\ 0.01,\ 0.1$ and 1. The data points represent numerical results from strict Bayesian analysis using the exact ground states of a double-well BEC, while the straight lines represent the asymptotical forms of Eq.(5) and Eq.(7), respectively.

In fact, almost any phase between $-\pi/2$ and $\pi/2$ can be measured at the maximum precision of $3.5/N$ if the present scheme is combined with multiple adaptive measurements [1, 7]. After the first measurement as described above, we can again rebalance the interferometer by adding θ_1/T to the tilt, followed by a second measurement with $\sigma_2 = \sigma_{min}(\Delta\theta_1, N)$, with result

n_2. The Bayesian distribution for θ_2 will then be approximately $P(\theta_2|n_2,n_1) \propto \exp[-(\theta_2-\bar{\theta}_2)^2/2y_2^2]$, where $\bar{\theta}_j = \sin^{-1}(2n_j/N)$ and $1/y_j^2 = \sum_{k=0}^{j} 1/\Delta\theta_k^2$. Since $\Delta\theta_j$ is much smaller than $\Delta\theta_{j-1}$ we can say $y_j \approx \Delta\theta_j \sim \Delta\theta_{min}(\Delta\theta_{j-1}, N)$. In other words, since the distribution after a measurement is much narrower than the previous distribution, multiplying the distributions has little effect, so that the final uncertainty is effectively determined by the resolution of the final measurement alone. After M iterations, with $\sigma_j = \sigma_{min}(\Delta\theta_{j-1}, N) \approx 0.57\,(N\tan\Delta\theta_0/2.1)^{3^{-j}}$, we find

$$\Delta\theta_M \sim (2.1/N)\,(N\tan\Delta\theta_0/2.1)^{3^{-M}}. \qquad (8)$$

While the above expressions are good estimates of the expected behavior, in practice each σ_j and $\Delta\theta_j$ would be computed exactly by applying Bayes theorem after each measurement. This procedure should be repeated only until $\Delta\theta_M \lesssim 10/N$, after which an addition measurement will push the phase uncertainty to $3.5/N$. The final measurement is then made using the GS state with $\sigma = 1$, which lies at the edge of the maximally-squeezed Fock regime defined by $\sigma \ll 1$. Thus an arbitrary phase can be measured at $3.5/N$ precision with $M+1$ measurements in total. Setting $\Delta\theta_M = 10/N$, and solving for M gives

$$M \approx 0.9\ln(\ln(N\tan\Delta\theta_0/2.1)) - 0.4, \qquad (9)$$

where again this is just an estimate subject to run-to-run fluctuations. For $\theta_r = \pi/3$ and $N = 10^4$, $M = 1.6$, i.e. only 2 or 3 total measurements will be required. For $N = 10^{12}$, $M = 2.6$, requiring 3 or 4 measurements. Even for $\Delta\theta_0$ extremely close to $\pi/2$, M remains small, for example, $\Delta\theta_0 = \pi/2 - 10^{-10}$ gives $M \approx 2.7$ for $N = 10^4$, and $M \approx 3.1$ for $N = 10^{12}$. Hence, for arbitrary phases in $(-\pi/2, \pi/2)$, our interferometer converges quickly to the $3.5/N$ precision within a few measurements, regardless of N. The final experimental value for the initial unknown phase is then $\theta = \sum_{j=1}^{M+1}\theta_j$ with a quantum-limited uncertainty of $\Delta\theta = 3.5/N$. The total number of atoms used to obtain this precision is $N_{tot} = (M+1)N$. For large enough N, we can approximate $\ln(N_{tot}/2(M+1)) \approx \ln(N_{tot})$, so that $M+1 \approx 0.9\ln(\ln(N_{tot}\tan\Delta\theta_0)) + 0.6$, which leads to the asymptotic scaling law

$$\Delta\theta \approx (2.1 + 3.2\ln(\ln(N_{tot}\tan\Delta\theta_0)))/N_{tot}. \qquad (10)$$

That the scaling law should depend on the initial phase interval has been previously pointed out [27]. As our final approximation effectively overestimates N_{tot}, the uncertainty approaches (10) from *below* as N increases.

In order to verify the accuracy of Eq. (9), as well as determine the magnitude of the run-to-run fluctuations, we have carried out exact Monte-Carlo simulations of many measurements of the phase $\pi/6$, with an initial uncertainty $\Delta\theta_0 = \pi/3$. During each simulation run, the measurement outcome was randomly selected according to the output distribution, and the phase information was determined numerically via Bayes theorem. The prescribed measure-rebalance process was iterated until the estimated phase uncertainty reaches $3.5/N$. Figure 3 shows the percentage of runs which attain the desired resolution on the $(M+1)$th iteration, for two different N values, with 10^4 runs each. The averages are $\overline{M+1} = 2.2$ for $N = 500$, and 2.5 for 5000. Equation (9) gives 2.2 and 2.5 as well. The corresponding variances $\Delta(M+1)$ are 0.4 and 0.6. We note that as the average approaches a half-integer value, the minimum possible variance approaches 0.5, because M is constrained to integer values. Thus the fluctuations are close to minimum allowed values.

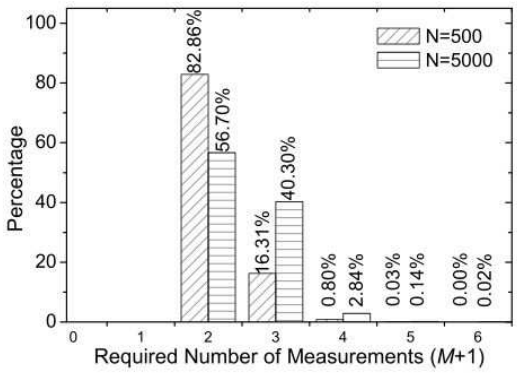

FIG. 3: Monte-Carlo simulation results showing the percentage of runs which achieved the maximum precision of $3.5/N$ after $(M+1)$ measurements, plotted versus $(M+1)$.

For TF and PS states, adaptive measurement schemes are extremely inefficient. This is due in part to their inability to distinguish positive from negative phases, which makes rebalancing impossible. But even if this were overcome, the primary difficulty is that the phase-uncertainty is N-independent for large phases, so that $\sim N^2$ measurements are required to obtain $1/N$ precision. This results in $1/N_{tot}^{1/3}$ scaling, worse than SQL.

The above discussions have assumed that the input state is optimally squeezed to width σ_{min}. A realistic input state, however, may deviate from σ_{min}, due to imprecise control over u and/or imprecise knowledge of N. A straightforward error analysis shows that our scheme is extremely robust against such uncertainties. The increase in the single-measurement phase uncertainty $\delta\Delta\theta$ due to fluctuations in u and N is found to be

$$\delta\Delta\theta = \left|\frac{\partial\Delta\theta(N,u)}{\partial N}\right|\delta N + \left|\frac{\partial^2\Delta\theta(N,u)}{\partial^2 u}\right|\frac{1}{2}\delta u^2 \qquad (11)$$

evaluated at $u = u_{min}$. The scaling with δu^2 reflects the fact that $u = u_{min}$ is a local minimum with respect to

the phase uncertainty. This gives

$$\delta\Delta\theta/\Delta\theta_{min} = (2/3)\delta N/N + (1/8)(\delta u/u_{min})^2, \quad (12)$$

so that a 10% variation in N leads to a 7% variation in the phase uncertainty, while even a 100% uncertainty in u only results in a 13% variation. For our purposes, these increases are essentially negligible, and are independent of the values of N or θ. Of course there are many other potential sources of error, e.g. the precision with which the tilt can be rebalanced, and the precision with which the scattering length can be set to zero during interferometer operation. Reaching the Heisenberg limit in a double-well BEC interferometer will clearly require major technological advances in many areas. Assuming that a level of precision significantly below the SQL is eventually obtained, the scheme we have developed will be the optimal method to obtain this precision, whether or not it is close to the Heisenberg limit.

In conclusion, we have shown that an adaptive GS state scheme has three advantages over previously discussed MZ interferometry schemes. It (1) can readily be implemented in a double-well BEC system, (2) can achieve a resolution well beyond the SQL for a wide range of phases with a single measurement, and (3) quickly converges to a final precision $\approx 10/N_{tot}$ with only a few adaptive measurements.

This work is supported in part by Nation Science Foundation Grant No. PHY0653373.

[1] B. Yurke, S. L. McCall, and J. R. Klauder, Phys. Rev. A. **33**, 4033 (1986).
[2] M. J. Holland and K. Burnett, Phys. Rev. Lett. **71**, 1355 (1993).
[3] P. Bouyer and M. A. Kasevich, Phys. Rev. A **56**, R1083 (1997).
[4] V. Giovannetti, S. Lloyd, and L. Maccone, Science **306**,1330 (2004).
[5] K. Eckert *et al*, Phys. Rev. A **73**, 013814 (2006).
[6] C. M. Caves, Phys. Rev. D **23**, 1693 (1981).
[7] D. Denot, T. Bschorr, and M. Freyberger, Phys. Rev. A **73**, 013824 (2006).
[8] L. Pezzé and A. Smerzi, Phys. Rev. Lett. **100**, 073601 (2008).
[9] J. J. Bollinger, Wayne M. Itano, D. J. Wineland, and D. J. Heinzen, Phys. Rev. A **54**, R4649 (1996).
[10] C. C. Gerry, Phys. Rev. A. **61**, 043811,(2000)
[11] W. J. Munro, K. Nemoto, G. J. Milburn, S. L. Braunstein, Phys. Rev. A **66**, 023819 (2002)
[12] S. F. Huelga *et al*, Phys. Rev. Lett. **79**, 3865 (1997).
[13] T. Schumm *et al*, Nature Physics **1**, 57 (2005).
[14] R. Gati *et al*, Appl. Phys. B **82** 207 (2006).
[15] G. -B. Jo *et al*, Phys. Rev. Lett. **98** 030407 (2007).
[16] C. Lee, Phys. Rev. Lett. **97**, 150402 (2006)
[17] L. Pezzé, A. Smerzi, G. P. Berman, A. R. Bishop, and L. A. Collins, Phys. Rev. A **74**, 033610 (2006).
[18] C.-S. Chuu *et al*, Phys. Rev. Lett. **95**, 260403 (2005).
[19] M. Shellekens *et al*, Science **310**, 648 (2005).
[20] Z. Hradil and J. Řeháček, Phys. Lett. A **334**, 267 (2005).
[21] L. Pezzé and A. Smerzi, e-print quant-ph/0508158 (2005).
[22] L. Pezzé and A. Smerzi, Phys. Rev. A **73**, 011801(R) (2006).
[23] H. Uys and P. Meystre, Phys. Rev. A **76**, 013804 (2007)
[24] T. Kim, *et al*, Phys. Rev. A, **57** 4004 (1998).
[25] A. Imamoḡlu, M. Lewenstein, and L. You, Phys. Rev. Lett. **78** 2511 (1997).
[26] L. Pezzé *et al*, Phys, Rev. A **72**, 043612 (2005).
[27] G. A. Durkin and J. P. Dowling, Phys. Rev. Lett. **99** 070801 (2007).